

Complexes of Uranyl Ions with Aromatic di- and tetra-Carboxylates Involving $[Ni(bipy)_n]^{2+}$ (n = 2, 3) Counter-Ions

Pierre Thuéry, Jack Harrowfield

▶ **To cite this version:**

Pierre Thuéry, Jack Harrowfield. Complexes of Uranyl Ions with Aromatic di- and tetra-Carboxylates Involving $[Ni(bipy)_n]^{2+}$ (n = 2, 3) Counter-Ions. European Journal of Inorganic Chemistry, 2017, 2017 (46), pp.5451-5460. 10.1002/ejic.201701086 . cea-01632567

HAL Id: cea-01632567

https://cea.hal.science/cea-01632567

Submitted on 10 Nov 2017

HAL is a multi-disciplinary open access archive for the deposit and dissemination of scientific research documents, whether they are published or not. The documents may come from teaching and research institutions in France or abroad, or from public or private research centers.

L'archive ouverte pluridisciplinaire **HAL**, est destinée au dépôt et à la diffusion de documents scientifiques de niveau recherche, publiés ou non, émanant des établissements d'enseignement et de recherche français ou étrangers, des laboratoires publics ou privés.

Complexes of Uranyl Ions with Aromatic di- and tetra-Carboxylates Involving $[Ni(bipy)_n]^{2+}$ (n = 2, 3) Counter-Ions

Pierre Thuéry*[a] and Jack Harrowfield*[b]

[a] NIMBE, CEA, CNRS, Université Paris-Saclay, CEA Saclay, 91191 Gif-sur-Yvette, France

E-mail: pierre.thuery@cea.fr

http://iramis.cea.fr/nimbe/

[b] ISIS, Université de Strasbourg, 8 allée Gaspard Monge, 67083 Strasbourg, France

E-mail: harrowfield@unistra.fr

https://isis.unistra.fr/

Keywords: Uranium(VI) / Aromatic carboxylic acids / Structure elucidation / Hirshfeld surface / Coordination networks

Abstract. Four di- and tetracarboxylate ligands based on aromatic platforms have been used to synthesize four uranyl ion complexes under solvo-hydrothermal conditions and in the presence of nickel(II) cations and 2,2'-bipyridine (bipy). The four complexes $[Ni(bipy)_3][(UO_2)_2(bdc)_3]\cdot 4H_2O$ (**1**, bdc^{2-} = 1,3-benzenedicarboxylate), $[Ni(bipy)_3][(UO_2)_2(ndc)_3]\cdot DMF\cdot 5H_2O$ (**2**, ndc^{2-} = 2,6-naphthalenedicarboxylate), $[UO_2(ntcma)(H_2O)_2]\cdot 2H_2O$ (**3**, $ntcma^{2-}$ = 1,4,5,8-naphthalenetetracarboxylate-1,8-monoanhydride), and $[UO_2Ni(hfdp)(bipy)_2(H_2O)]\cdot H_2O$ (**4**, $hfdp^{4-}$ = 4,4'-(1,1,1,3,3,3-hexafluoroisopropylidene)diphthalate) crystallize as two-dimensional assemblies. While separated $[Ni(bipy)_3]^{2+}$ counter-ions are present in **1** and **2**, the $Ni(bipy)_2^{2+}$ groups in **4** are bound to carboxylate donors and are decorating species on the polymeric network, while nickel(II) is absent in the neutral complex **3**. The networks in **1**–**3** have the $\{6^3\}$ hcb topology and that in **4** the $\{4.8^2\}$ fes one. Apart from Coulombic interactions in **1** and **2**, OH···O and CH···O hydrogen bonds are prominent interactions in the lattices, as shown by Hirshfeld surface analysis. Uranyl emission spectra in **1** and **4**, in spite of almost complete quenching in the former, are in agreement with those measured in other polycarboxylate complexes with six and five equatorial donors, respectively.

Introduction

Aromatic mono- and polycarboxylates, not only the simplest ones based on benzene or pyridine rings, but also those containing connected or fused rings, are staple ligands in the design of uranyl–organic coordination polymers and frameworks.[1–3] Considering the number of available aromatic platforms, the many possible locations of carboxylate groups on them, and their potential additional functionalization, the structural variety in this family of ligands is huge. Therefore, it is no wonder that, combined with a variety of experimental conditions and additional metal cations or co-ligands, it has resulted in the synthesis of a very large number of uranyl complexes, as witnessed by the presence of more than 450 crystal structures in the Cambridge Structural Database (CSD, Version 5.38).[4] In the last few years, we have been particularly interested in the use of $[M(L)_n]^{+/2+}$ [where M is a d-block metal cation, n = 2 or 3, L = 2,2′-bipyridine (bipy) or 1,10-phenanthroline (phen)] as counter-ions for anionic uranyl-containing species, a strategy which has proven particularly rewarding with polycarboxylates based on aliphatic or alicyclic skeletons.[5–11] There are also several cases, either from other groups,[12–16] or from ours,[17–22] of association of these counter-ions (sometimes not separately but also bound to the carboxylate ligand) with uranyl complexes based on aromatic ligands.

Solvothermal reaction conditions most commonly lead to the crystallisation of uranyl ion complexes of the fully deprotonated polycarboxylic acid. Species based on the neutral $UO_2(carboxylate)_2$ unit are thus readily obtained but addition of a second cation to reaction mixtures, often otherwise of the same composition, can lead to crystallisation of heterometallic species based on the anionic $[UO_2(carboxylate)_3]^-$ unit. The exact nature of the heterometallic

complex lattice depends upon both the particular heterometal ion and its coordination environment. Where this coordination environment is such as to exclude binding to carboxylate, the heterometal ion must exert its influence through secondary coordination sphere interactions and while we have had very limited success in the use of cationic complexes capable of NH···O bonding (for example, $[Co(en)_3]^{3+}$, where en is ethylenediamine[10]), the use of those, typically $[M(bipy)_3]^{2+}$ or $[M(phen)_3]^{2+}$, capable of CH···O bonding, has been much more fruitful, leading, for example, to the first examples of triple helicate species involving uranium.[7] In exploration of some reaction systems with various ratios of heterometal ion to bipy or phen in the initial mixture, more complicated materials have been obtained where the coordination sphere of the metal is only partially blocked by the diimine ligand and either carboxylate binding or the retention of hydrogen bonding aqua ligands occurs.

To assess such behaviour in greater detail, we have synthesized three novel compounds from 1,3-benzenedicarboxylic acid (or isophthalic acid, H_2bdc), 2,6-naphthalenedicarboxylic acid (H_2ndc), and 4,4'-(1,1,1,3,3,3-hexafluoroisopropylidene)diphthalic acid (H_4hfdp), which all involve $[Ni(bipy)_n]^{2+}$ (n = 2 or 3) counter-ions. The crystal structures of these complexes have been determined, as well as that of a neutral uranyl complex obtained from 1,4,5,8-naphthalenetetracarboxylic acid (H_4ntc) under analogous conditions, and the uranyl emission spectra of two of them have been measured. Isophthalic acid is a common enough ligand for uranyl, with eleven crystal structures reported in the CSD,[23–31] which are either molecular,[28,30] one-,[23,27] two-,[27,31] or three-dimensional.[24–26,29] No uranyl complex with either of the two naphthalene derivatives has been reported (but nine structures with the positional isomer 1,4-naphthalenedicarboxylate are in the CSD[13,32–35]). Uranyl complexation by 4,4'-(1,1,1,3,3,3-

hexafluoroisopropylidene)diphthalic acid has been the subject of only one study,[36] three complexes with the geometrically related benzophenone-3,3',4,4'-tetracarboxylic acid having also been reported.[37,38]

Results and Discussion

Syntheses

All complexes were synthesized under solvo-hydrothermal conditions (140 °C, autogenous pressure). Ni^{II} was used as additional cation in all cases; this ion constitutes a convenient choice from the first row transition metal ions since its complexes are more stable than those of Mn^{II}, the stability constants for its bipy and phen complexes follow a "normal" order unlike those for Fe^{II}, enabling predominance of mono-, bis- and tris-diimine species under appropriate conditions, and it is less prone to redox reactions such as may occur with Co^{II} and Cu^{II}. Several organic co-solvents were tested for each of the four carboxylic acids used, and those which have given crystalline species suitable for structure determination happen to be different in all four cases, being either tetrahydrofuran (THF), *N,N*-dimethylformamide (DMF), acetonitrile, or *N*-methyl-2-pyrrolidone (NMP), all potentially coordinating species, for **1**–**4**, respectively. However, in no case is the co-solvent present in the final compound as a co-ligand, and only in complex **2** is DMF retained as a lattice solvent (as well as possibly, from the elemental analysis results, CH_3CN in **3**). Concerning the syntheses, the most unexpected result here is that of complex **3**, prepared from 1,4,5,8-naphthalenetetracarboxylic acid (H_4ntc), but containing instead just its doubly deprotonated 1,8-monoanhydride ($ntcma^{2-}$). Anhydrides are commonly hydrolyzed under hydrothermal conditions,[37,38] but the six-membered ring formed here enhances the stability of

the anhydride unit. Another index of this stability is that recrystallization of H_4ntc from dimethyl sulfoxide gives crystals of the monoanhydride.[39] It may be noted, however, that complex **3** was only obtained in low yield, together with an amorphous powder which was not further characterized, and that it probably does not represent the dominant species in solution.

Crystal Structures

The complex $[Ni(bipy)_3][(UO_2)_2(bdc)_3]\cdot 4H_2O$ (**1**) crystallizes in the orthorhombic space group *Pnna*, with one uranium atom, two bdc^{2-} ligands (one of them with twofold rotation symmetry) and one counterion, also with twofold rotation symmetry, in the asymmetric unit (Figure 1). The uranyl cation is chelated by three carboxylate groups, the uranium atom being thus in the usual hexagonal bipyramidal environment [U–O(oxo) bond lengths 1.768(4) and 1.784(4) Å, U–O(carboxylate) 2.448(3)–2.487(4) Å], and the geometry of the octahedral $[Ni(bipy)_3]^{2+}$ cation is unexceptional [Ni–N bond lengths 2.070(4)–2.105(4) Å]. The uranium atom is a threefold node and its ligands simple links in the two-dimensional (2D) assembly parallel to (0 1 0) which is formed. This network has the point (Schläfli) symbol $\{6^3\}$ and the honeycomb topological type. Due to the shape of the ligands, which point alternately inside and outside the hexagonal cell, the latter assumes in fact a distinctly triangular outline, at variance with the regular hexagonal net obtained with 1,4-benzenedicarboxylate (terephthalate).[16,32] Hexanuclear elongated cells are obtained in two uranyl complexes with bis-chelating bdc^{2-} ligands which crystallize as one-dimensional ribbons, the presence of water ligands probably preventing higher dimensionality polymerization in these cases.[23,27] Neither of the two 2D assemblies reported with this ligand, of

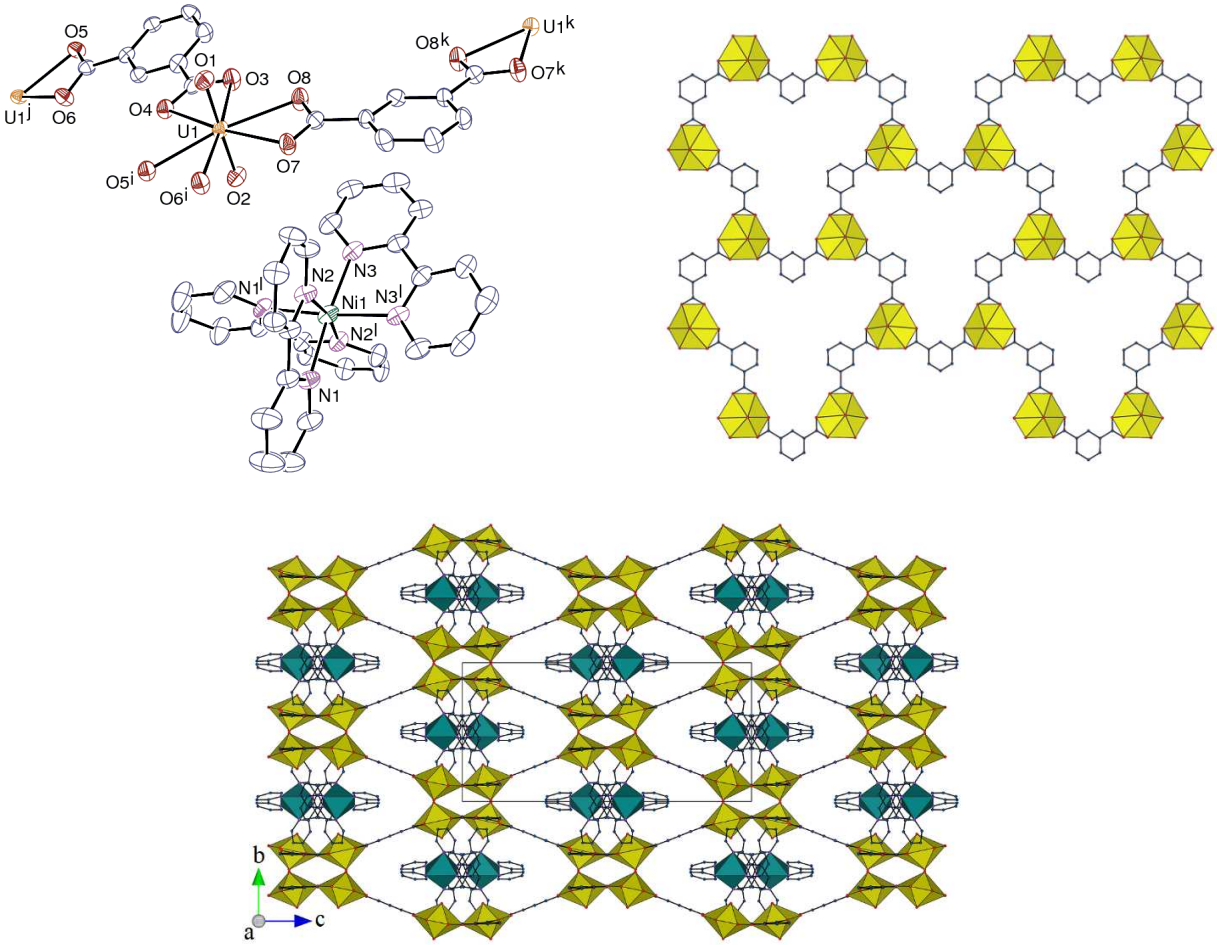


Figure 1. Top left: view of complex **1**. Displacement ellipsoids are drawn at the 50% probability level. Symmetry codes: i = *x* + 1/2, *y*, 1 – *z*; j = *x* – 1/2, *y*, 1 – *z*; k = *x*, 1/2 – *y*, 1/2 – *z*; l = 3/2 – *x*, –*y*, *z*. Top right: view of the 2D network. Bottom: view of the packing with sheets viewed edge-on; uranium coordination polyhedra are colored yellow and those of nickel(II) green. The solvent molecules and hydrogen atoms are omitted in all views.

the bilayer type with propane-1,3-diammonium,[27] or $[Co(H_2O)_6]^{2+}$ counter-ions,[31] displays a topology similar to that of **1**. The zigzag section of the sheets in **1**, when viewed down the *a* axis, results in the formation of flattened channels in the lattice, in which the counter-ions are located, the arrangement being quite compact, with a Kitaigorodski packing index (KPI, estimated with PLATON[40]) of 0.52, with disordered solvent molecules excluded. Viewed down the *a* axis, the

cations project as pairs enclosed by undulations within the anionic polymer sheets and this is actually a projection of a zig-zag column in which the chirality alternates. The aromatic rings of both carboxylate ligands are possibly involved in parallel-displaced π-stacking interactions, one with its image through a twofold rotation axis pertaining to an adjacent layer, which corresponds to the region of closest inter-layer contact [centroid···centroid distance 3.661(3) Å, dihedral angle 2.2(2)°], and the other with two bipyridine aromatic rings located on either side of it [centroid···centroid distance 3.939(3) Å, dihedral angle 18.3(2)°]. However, these interactions do not appear prominently on the Hirshfeld surface (HS)[41] calculated with CrystalExplorer[42] (Figure 2). Hirshfeld surfaces provide in essence a map of the van der Waals (vdW) surface of the molecular unit chosen, and allow the visualization of any intermolecular interaction which exceeds dispersion forces; these specific interactions are indicated by a red (and in a lesser degree white) coloration on the surface of the HSs mapped with d_{norm}, the latter being a combination of the distances d_i and d_e to the surface of the nuclei located inside and outside of it, taking into account their van der Waals radii. In contrast, the blue coloration indicates the absence of contacts shorter than or equal to the sum of vdW radii. The associated 2D fingerprint plots give a representation of the fraction of surface points involved for each (d_i, d_e) pair, with colors ranging from dark blue (few points) to brighter colors and finally red (many points); they provide a way of identifying particular interacting atoms inside and outside the Hirshfeld surface by their distances from the surface and thus from one another. No CH···π interaction is present in **1**, but four weak CH···O hydrogen bonds[43,44] connect hydrogen atoms of the cation and oxo (O2, involved in three bonds) and carboxylato (O7) groups of the anion [C···O distances 3.127(7)–3.467(7) Å, H···O 2.45–2.54 Å, C–H···O angles 128–178°], and they appear conspicuously on the fingerprint plot and the

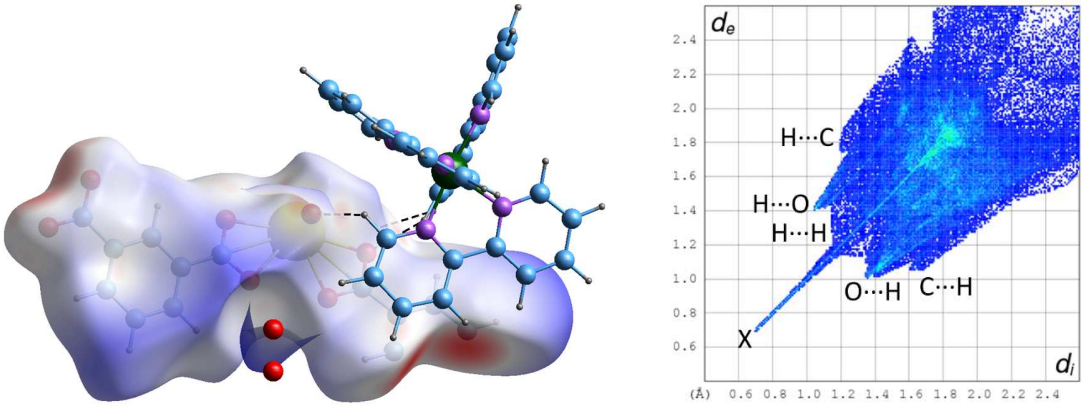


Figure 2. Left: Hirshfeld surface mapped with d_{norm} calculated on the anionic part of the asymmetric unit of complex **1**. Hydrogen bonds are shown as dashed lines. The large red spots on the left and the bottom right are due to truncation of the polymer chain. Isolated oxygen atoms are water molecules for which hydrogen atoms were not located. Right: fingerprint plot with interactions indicated with the atom located inside the HS first. The spike indicated by an X is an artefact due to truncation of C–C bonds at the border of the asymmetric unit.

HS, of which O···H contacts represent overall about 33%. The fact must be stressed that such interactions bring only a very small contribution to the stability of the lattice, which is predominantly due to Coulombic forces,[45] and they can at best account for some of the finest local details.

The complex with the naphthalene dicarboxylate derivative, $[Ni(bipy)_3][(UO_2)_2(ndc)_3]\cdot DMF\cdot 5H_2O$ (**2**), crystallizes in the monoclinic space group $P2_1/n$, with two independent uranyl ions, three ndc^{2-} ligands and one $[Ni(bipy)_3]^{2+}$ counter-ion in the asymmetric unit (Figure 3). Here also, the uranium atoms are chelated by three carboxylate groups, and all bond lengths are unexceptional [U–O(oxo) 1.769(4)–1.778(4) Å, U–O(carboxylate) 2.442(3)–2.497(3) Å, Ni–N 2.069(4)–2.102(4) Å]. A honeycomb 2D network parallel to (2 0 1) is formed, which displays a much more regular arrangement than that in **1** due to the linear shape of the

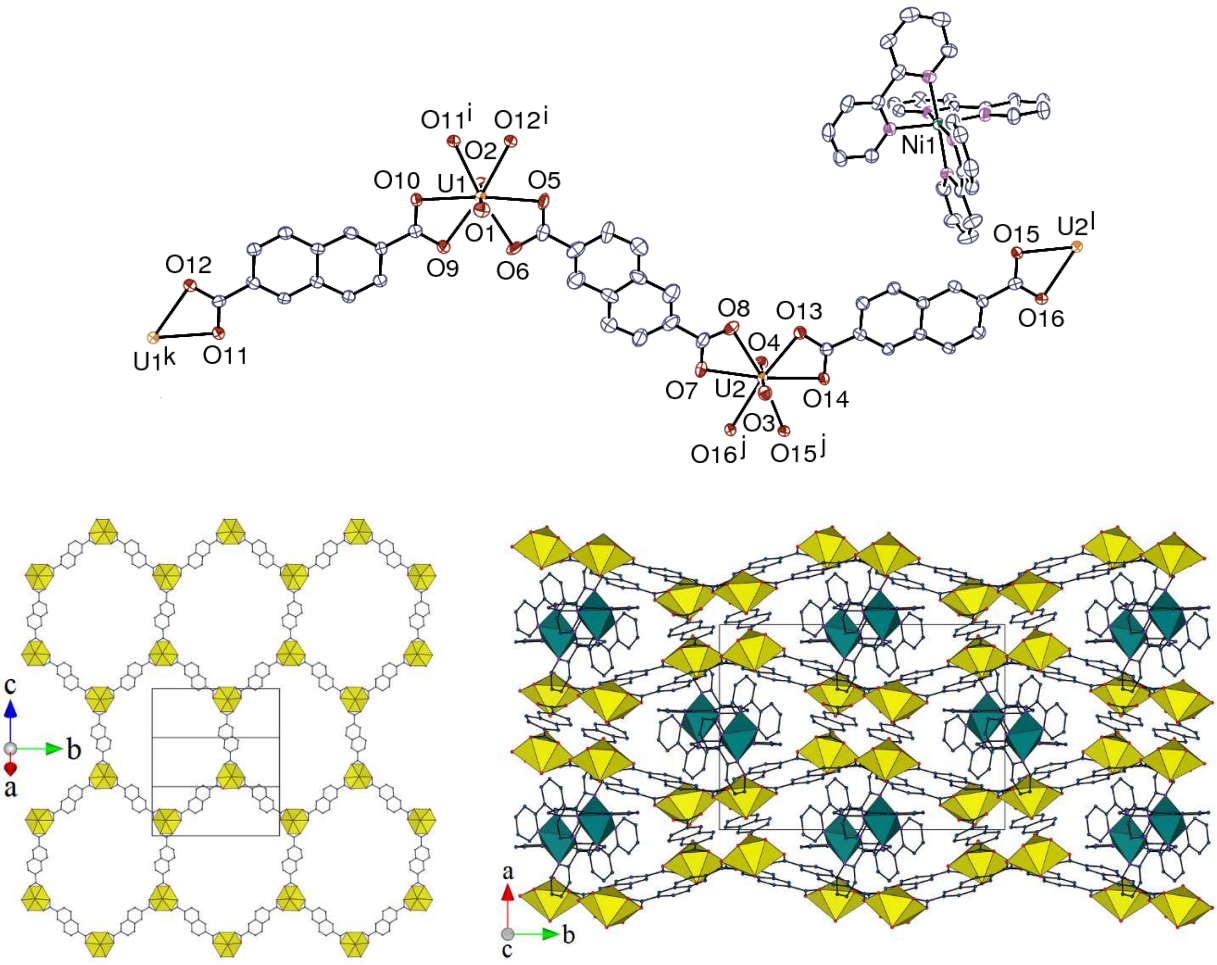


Figure 3. Top: view of complex **2**. Displacement ellipsoids are drawn at the 50% probability level. Symmetry codes: i = 3/2 – *x*, *y* + 1/2, –*z* – 1/2; j = 1/2 – *x*, *y* – 1/2, 3/2 – *z*; k = 3/2 – *x*, *y* – 1/2, –*z* – 1/2; l = 1/2 – *x*, *y* + 1/2, 3/2 – *z*. Bottom right: view of the 2D network. Bottom left: view of the packing with uranium coordination polyhedra colored yellow and those of nickel(II) green. The solvent molecules and hydrogen atoms are omitted in all views.

ligand (the honeycomb topology is also obtained with the positional isomer 1,4-naphthalenedicarboxylate and potassium or guanidinium counter-ions[32]). The hexagonal cells in **2** have largest and smallest dimensions of ~24 and 18 Å (or ~29 and 26 Å between metal centres), which would be suitable for network entanglement, as observed with other divergent ditopic ligands giving analogous honeycomb networks, with comparable or even smaller

dimensions.[8,21,22,32,46] However, this is not so here, and the planar sheets with their counter-ions are stacked in a regular fashion (KPI 0.71, or 0.61 with solvent excluded). Channels with the same shape as those in **1** run along the *c* axis and contain, in alternation, both enantiomers of the counter-ions, but they are here inclined with respect to the sheets, and not parallel to the sheet plane as in **1**. Analysis of short contacts indicates that several parallel-displaced π-stacking interactions may be present, between rings of carboxylate ligands pertaining to different layers, or rings from carboxylate ligands and bipy, and also between two bipy rings [centroid···centroid distances 3.654(3)–4.368(3) Å, dihedral angles 0–26.1(3)°]. Three CH···π interactions may be present as well, between hydrogen atoms of ndc^{2-} and bipy rings, or the reverse [H···centroid 2.92–3.00 Å, C–H···centroid 130–164°]. Most prominent on the HS (Figure 4), on which they appear as red dots, are however the OH···O and CH···O hydrogen bonds. The lattice water molecules for which the hydrogen atoms were located (see Experimental Section) are hydrogen bonded to oxo or carboxylato oxygen atoms, or other water molecules [O···O 2.818(6)–3.282(5) Å, H···O 2.00–2.47 Å, O–H···O 130–166°]. Seven CH···O hydrogen bonds may also be present, between bipy hydrogen atoms and oxo, carboxylato or water oxygen atoms [C···O 3.107(6)–3.525(7) Å, H···O 2.28–2.59 Å, C–H···O 143–170°]; overall, O···H contacts represent about 39% of the HS.

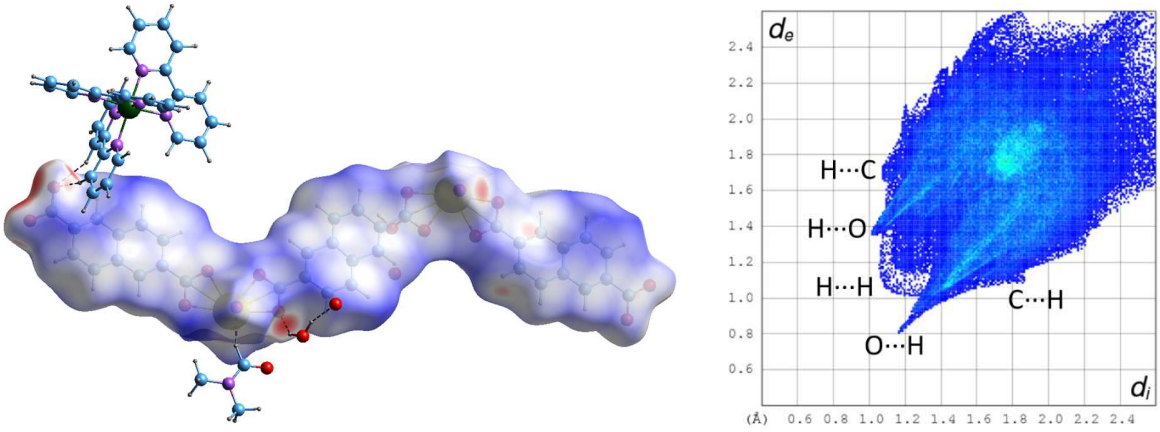


Figure 4. Left: Hirshfeld surface mapped with d_{norm}, calculated on the anionic part of the asymmetric unit of complex **2**. Hydrogen bonds are shown as dashed lines (the isolated red atom corresponds to a water molecule for which the hydrogen atoms were not located). The large red dot on the left is due to truncation of the polymer chain. Right: fingerprint plot with interactions indicated with the atom located inside the HS first.

Complex **3**, $[UO_2(ntcma)(H_2O)_2]\cdot 2H_2O$, is a homometallic, neutral species which involves $ntcma^{2-}$, the monoanhydride of ntc^{2-}. It crystallizes in the monoclinic space group $P2_1/c$, with one uranyl cation, one $ntcma^{2-}$ ligand and four water molecules, two of them coordinated, in the asymmetric unit (Figure 5). The uranium atom is bound to three carboxylate oxygen atoms from three different ligands and two water molecules, and the uranium environment is thus pentagonal bipyramidal [U–O(oxo) 1.762(3) and 1.764(3) Å, U–O(carboxylate) 2.336(3)–2.412(3) Å, U–O(water) 2.406(3) and 2.462(3) Å]. The carboxylate groups are either monodentate (κ^1O) or bridging bidentate (μ_2-κ^1O:κ^1O'); the fused rings are planar with a rms deviation of 0.13 Å, and the two carboxylate groups make dihedral angles of 31.7(4) and 59.0(2)° with this plane, and 46.8(5)° with each other [42.7(1), 56.4(1) and 32.4(4)°, respectively, in the uncomplexed H_2ntcma[39]]. Both metal and ligand are threefold nodes in the 2D network parallel to (0 0 1) which is formed, with here also the honeycomb topology, although the hexagonal cells are much smaller

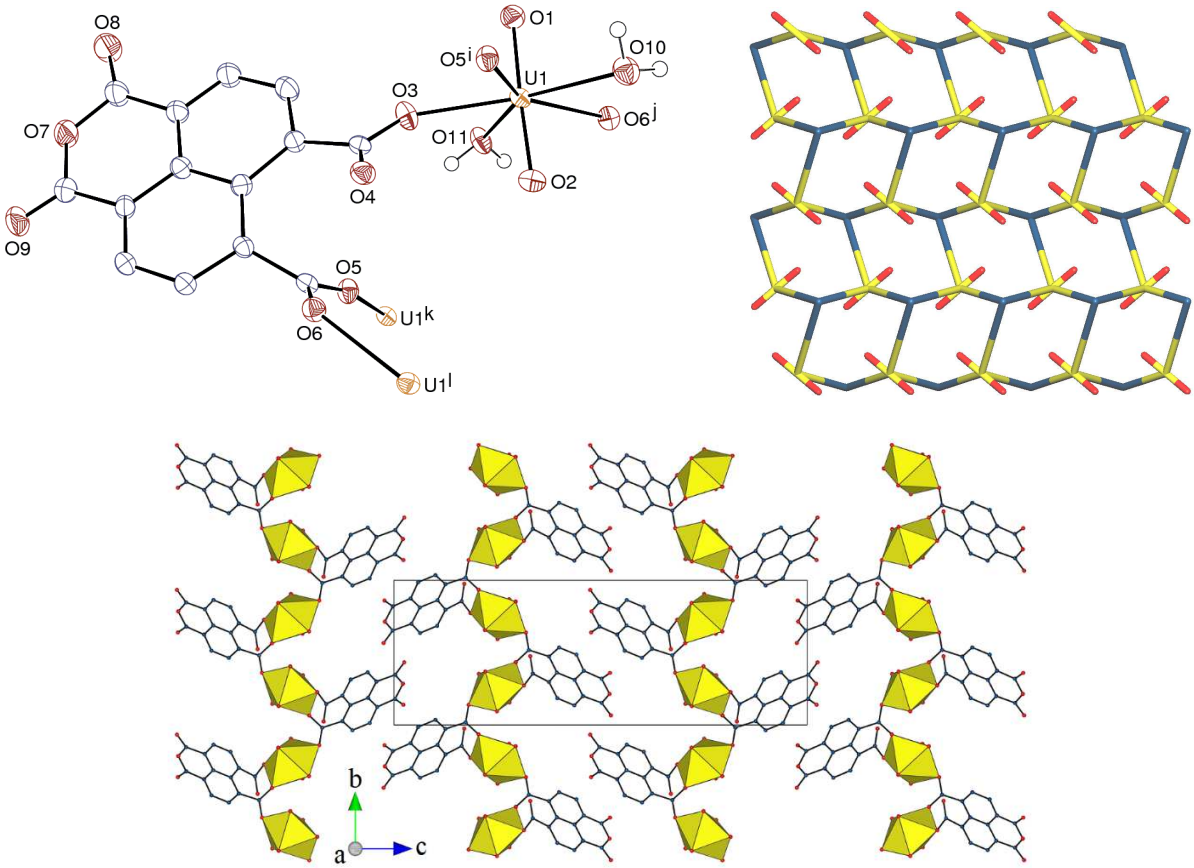


Figure 5. Top left: view of complex **3**. Displacement ellipsoids are drawn at the 50% probability level. The solvent molecules and carbon-bound hydrogen atoms are omitted. Symmetry codes: i = *x* – 1, *y*, *z*; j = 1 – *x*, *y* + 1/2, 3/2 – *z*; k = *x* + 1, *y*, *z*; l = 1 – *x*, *y* – 1/2, 3/2 – *z*. Top right: simplified view of the 2D network (yellow: uranium, red: oxygen, blue: centroid of the dicarboxylate ligand). Bottom: packing with sheets viewed edge-on; uranium coordination polyhedra are colored yellow and the solvent molecules and hydrogen atoms are omitted.

(~6 Å in their largest dimension) than in the two previous cases since they contain three metal and three ligand nodes instead of six metal nodes and six ligand links as in **1** and **2**. The cells are also very distorted, a consequence of the irregular bonding mode and the presence of the very bulky ligand skeletons which point outwards on the two sides of the sheets. The compact packing

(KPI 0.74, or 0.65 with solvent excluded) displays interdigitation of the layers, and analysis of short contacts indicate that two parallel-displaced π-stacking interactions may be present, albeit the rings are quite distant [centroid···centroid distances 4.349(2) and 4.389(2) Å, dihedral angles 1.95(19) and 2.45(19)°], but examination of the HS (Figure 6) shows that they are not greater than dispersion. The parallel geometry of all rings does not enable CH···π interactions, but OH···O and CH···O hydrogen bonds are present. Each of the two anhydride oxygen atoms O8 and O9 in particular is involved in a hydrogen bond with a solvent water molecule [O···O 2.994(6) and 3.008(6) Å, H···O 2.07 and 2.09 Å, O–H···O 164 and 167°, respectively], and also in weaker CH···O hydrogen bonds involving donors in the carboxylate-bearing rings from adjacent units [C···O 3.236(6) and 3.255(5) Å, H···O 2.37 and 2.33 Å, C–H···O 151 and 165°, respectively]. All these hydrogen bonds appear prominently in the HS and in the corresponding fingerprint plot; overall,

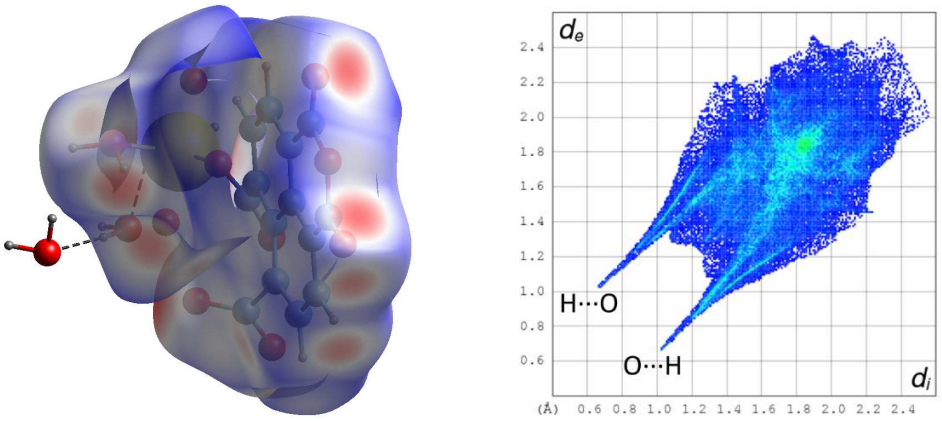


Figure 6. Left: Hirshfeld surface mapped with d_{norm} calculated on the asymmetric unit of complex **3**. Hydrogen bonds are shown as dashed lines. The red dots on the front correspond to OH···O and CH···O hydrogen bonds involving anhydride oxygen atoms. Right: fingerprint plot with interactions indicated with the atom located inside the HS first.

O···H interactions represent 47% of the HS. It is also notable that atom O9 is at distances of 3.424(4)–3.933(4) Å from the centroids of aromatic rings located on either side of the group to which it pertains, but these contacts appear to be no greater than dispersion in the HS.

The only tetracarboxylate complex in this series, $[UO_2Ni(hfdp)(bipy)_2(H_2O)]\cdot H_2O$ (**4**), crystallizes in the triclinic space group $P\bar{1}$ with an asymmetric unit containing two crystallographically independent, but nearly identical moieties (Figure 7). This complex is

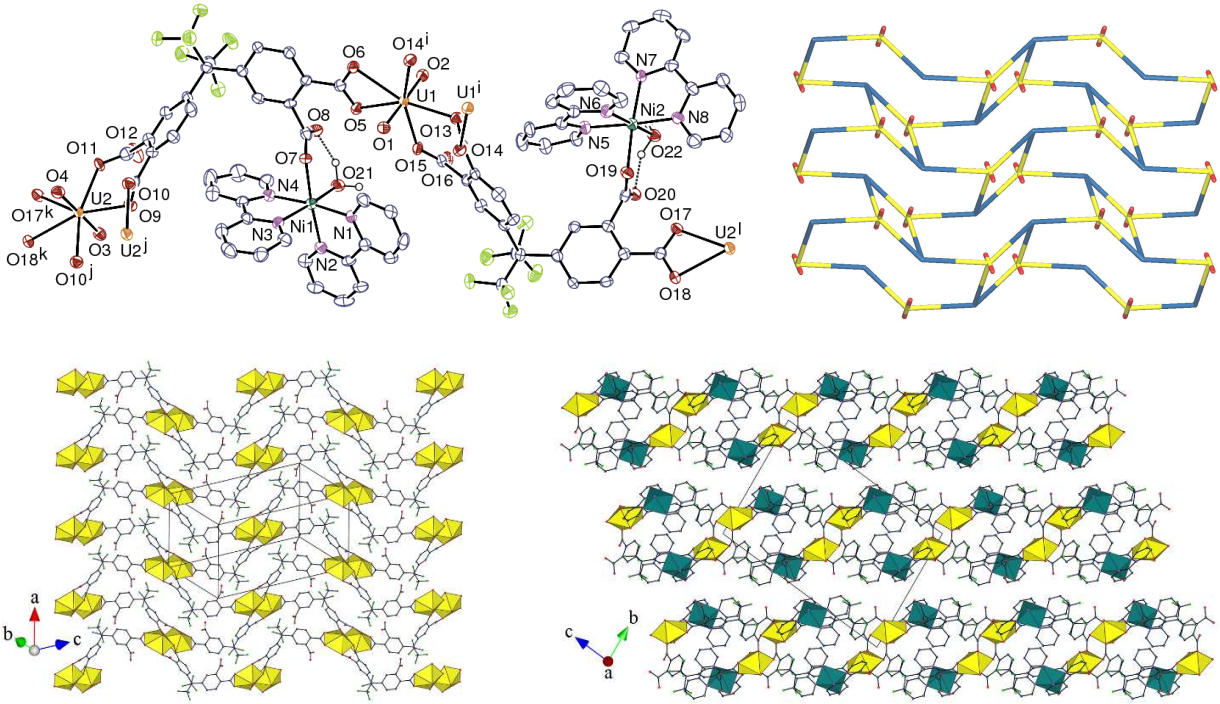


Figure 7. Top left: view of complex **4**. Displacement ellipsoids are drawn at the 50% probability level. Solvent molecules and carbon-bound hydrogen atoms are omitted. Hydrogen bonds are shown as dashed lines. Symmetry codes: i = 1 – *x*, 1 – *y*, 1 – *z*; j = 2 – *x*, 2 – *y*, –*z*; k = *x*, *y* + 1, *z* – 1; l = *x*, *y* – 1, *z* + 1. Top right: simplified view of the 2D network (yellow: uranium, red: oxygen, blue: centroid of the tetracarboxylate ligand). Bottom left: view of the 2D network with $Ni(bipy)_2^{2+}$ groups omitted. Bottom right: packing with sheets viewed edge-on. Uranium coordination polyhedra are colored yellow and those of nickel(II) green; solvent molecules and hydrogen atoms are omitted in the last two views.

different from **1** and **2** in that the *cis*-Ni(bipy)$_2^{2+}$ counter-ion is not isolated, but bound to a carboxylate group, a situation which is rather common with M(bipy/phen)$_n$ (n = 1 or 2) groups.[6–8,10–12,17,20,47–53] Incorporation of additional metal cations within uranyl-containing coordination polymers is often used to reach dimensionality increase, but the presence of *N*-chelating species such as bipy or phen severely restricts this possibility. Both uranium atoms in **4** are in pentagonal bipyramidal environments, being chelated by one carboxylate group from one ligand, and bound to two carboxylate groups from a second ligand and another one from a third ligand [U–O(oxo) 1.761(5)–1.769(5) Å, U–O(carboxylate) 2.286(5)–2.395(5) Å and 2.414(5)–2.486(5) Å for monodentate and chelating groups, respectively]. The nickel(II) cations are chelated by two bipy molecules and bound to one carboxylate group in monodentate fashion, and one water molecule, the environment being octahedral in a *cis*-NiN_4O_2 arrangement [Ni–N 2.034(6)–2.095(6) Å, Ni–O(carboxylate) 2.088(5) and 2.079(5) Å, Ni–O(water) 2.062(5)–2.081(5) Å]. Each ligand is bound to three uranium and one nickel(II) atoms, the carboxylate groups having the coordination modes κ^1O (twice, with one oxygen atom left uncoordinated in each case), κ^2O,O', and μ_2-κ^1O:κ^1O'. Both uranium and hfdp^{4-} are thus threefold nodes, while Ni(bipy)$_2^{2+}$ does not contribute to polymerization and is a mere decorating group. This group is chiral, however, and the two independent ligands are bound to enantiomeric Ni(bipy)$_2^{2+}$ units. The 2D assembly formed, parallel to (0 1 1), has the point symbol {4.8^2} and the common fes topological type. The sheets, planar and with a thickness of ~12 Å, are packed so as to leave no significant channel (KPI 0.67, or 0.65 with solvent excluded). The complex formed by hfdp^{4-} with uranyl ions alone crystallizes also as a thick 2D network, but in this case the uranyl cations are located on the faces and the

ligands span the whole inner space,[36] while the sheets in **4** can be seen as built of two thin layers connected to one another by the bridging bidentate carboxylate groups. It is notable that thick, bilayer arrangements were also found in uranyl ion complexes of the related ligand benzophenone-3,3',4,4'-tetracarboxylate,[37,38] suggesting a particular propensity of these V-shaped ligands to form such architectures. In this case also, parallel-displaced π-stacking interactions involving both ligands may be present, [centroid···centroid distances 3.836(5)–4.434(5) Å, dihedral angles 0–14.1(4)°], but examination of the HS shows that they are not greater than dispersion. Two possible CH···π interactions involving hydrogen atoms from $hfdp^{4-}$ and bipy molecules are found [H···centroid 2.79 and 2.83 Å, C–H···centroid 139 and 138°]. The lattice water molecules are hydrogen bonded to each other and to carboxylate oxygen atoms (mainly the uncoordinated ones) [O···O 2.584(7)–3.068(7) Å, H···O 1.66–2.33 Å, O–H···O 128–174°] and CH···O hydrogen bonds between bipy hydrogen atoms and oxo, carboxylato and water oxygen atoms are also present [C···O 3.138(10)–3.593(9) Å, H···O 2.47–2.65 Å, C–H···O 118–171°]. All these hydrogen bonds appear prominently on the HS (Figure 8), and the O···H contacts represent overall 24% of the surface, the fingerprint plot displaying also a notable central H···H feature (21%) and two lateral C···H ones (14%). Half the CF_3 groups are located on the surfaces of the layers, but only one inter-layer F···F short contact, at 2.94 Å, is found, and, both from what is known of such interactions,[54] and from examination of the HS, it can be concluded that this has no stabilizing effect on the packing. It may be noted however that halogen···halogen interactions, with halogens heavier than fluorine, have recently been used successfully in the design of uranyl–organic assemblies.[55–57]

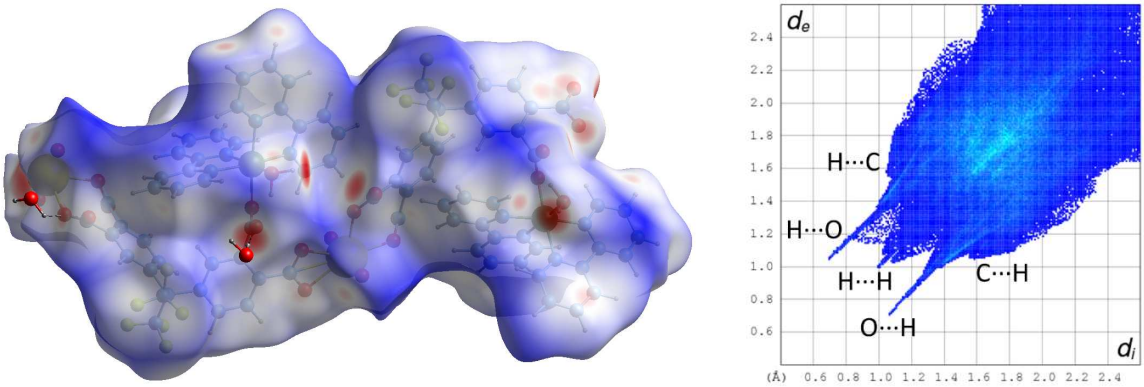


Figure 8. Left: Hirshfeld surface mapped with d_{norm} calculated on the asymmetric unit of complex **4**. Hydrogen bonds are shown as dashed lines. The red dots on the front correspond to OH···O and CH···O hydrogen bonds. Right: fingerprint plot with interactions indicated with the atom located inside the HS first.

Luminescence Properties

The emission spectra of complexes **1** and **4** in the solid state were recorded at room temperature under excitation at a wavelength of 420 nm, a value suitable for excitation of the uranyl chromophore,[58] and they are shown in Figure 9. The intense and well-resolved spectrum of **4** shows the typical vibronic progression corresponding to the $S_{11} \rightarrow S_{00}$ and $S_{10} \rightarrow S_{0\nu}$ (ν = 0–4) electronic transitions,[59] while the weak spectrum of **1** displays only three badly resolved peaks, uranyl emission being quenched as frequently observed when d-block metal cations provide nonradiative relaxation pathways.[60] The main maxima in the spectrum of **4** are at 474, 491, 512, 535, 560 and 588 nm, and the two most discernible maxima in the spectrum of **1** are at 481 and 499 nm (these corresponding to the second and third maxima of **4**). These values are in agreement with those generally measured in uranyl carboxylate complexes with seven- and eight-coordinate uranium environments,[61] respectively, the former being redshifted by about 10 nm with respect to the latter in the present case. Such a redshift is probably attributable to an

increase in donor strength of the ligands in the equatorial plane which induces a decrease in uranyl oxo bond order.[62,63] The average vibronic splitting energy for the $S_{10} \rightarrow S_{0\nu}$ transitions in **4** is 840 cm^{-1}, a value in the usual range.[59,61,64–66]

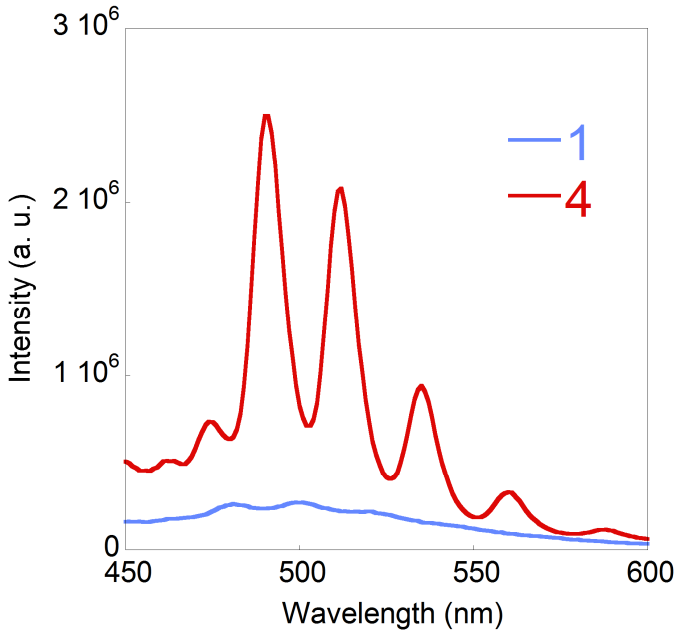


Figure 9. Solid state emission spectra of complexes **1** and **4**, measured with an excitation wavelength of 420 nm.

Conclusions

The structures described herein of four novel uranyl ion complexes synthesized under solvo-hydrothermal conditions in the presence of additional nickel(II) cations and 2,2'-bipyridine, and involving four different di- and tetracarboxylate ligands based on aromatic platforms, illustrate some of the versatility of Ni^{II} as a counter-cation influencing the nature of the uranyl ion coordination polymer formed. In two cases (complexes **1** and **2**) the $[Ni(bipy)_3]^{2+}$ cation is present as a counter-ion for the anionic uranyl-containing polymer in the final crystalline compound, while the *cis*-$Ni(bipy)_2^{2+}$ group is appended to the polymer in **4**, and both nickel(II) and bipy are absent

in **3** (this complex containing the monoanhydride of the tetracarboxylate used). All four complexes crystallize as 2D assemblies, three of them with honeycomb and the fourth with fes topology, but, although large hexanuclear cells are formed in **2**, no network entanglement is observed. In comparison to the cases where uranyl complexes with the same ligands had previously been obtained under different experimental conditions, the topologies observed here are different, thus evidencing the structure-directing effect of the nickel(II)-containing moieties, but these are cases in which use of an additional metal ion fails to increase the dimensionality to 3D, or promote intricate entangled structures. The emission spectra measured in the solid state for complexes **1** and **4** (that for **1** being largely quenched) give maxima positions in agreement with those measured for a series of uranyl carboxylate complexes with six or five equatorial donors, the maxima of the former being blueshifted with respect to those of the latter.

Experimental Section

General: $UO_2(NO_3)_2 \cdot 6H_2O$ (depleted uranium, R. P. Normapur, 99%), and $Ni(NO_3)_2 \cdot 6H_2O$ were purchased from Prolabo, 1,3-benzenedicarboxylic acid (H_2bdc), 2,6-naphthalenedicarboxylic acid (H_2ndc), 1,4,5,8-naphthalenetetracarboxylic acid (H_4ntc), 4,4'-(1,1,1,3,3,3-hexafluoroisopropylidene)diphthalic acid (H_4hfdp) were from Aldrich, and 2,2'-bipyridine (bipy) was from Fluka. Elemental analyses for compounds **1**, **3** and **4** were performed by MEDAC Ltd. at Chobham, UK. A similar analysis could not be conducted for compound **2** due to the low yield of the synthesis.

Caution! *Uranium is a radioactive and chemically toxic element, and uranium-containing samples must be handled with suitable care and protection.*

$[Ni(bipy)_3][(UO_2)_2(bdc)_3]\cdot 4H_2O$ (1): 1,3-benzenedicarboxylic acid (17 mg, 0.10 mmol), $UO_2(NO_3)_2\cdot 6H_2O$ (50 mg, 0.10 mmol), $Ni(NO_3)_2\cdot 6H_2O$ (15 mg, 0.05 mmol), 2,2′-bipyridine (24 mg, 0.15 mmol), tetrahydrofuran (0.2 mL), and demineralized water (0.6 mL) were placed in a 15 mL tightly closed glass vessel and heated at 140 °C under autogenous pressure, giving light orange crystals of complex **1** within one week (47 mg, 86% yield based on the acid). Elemental analysis results are consistent with the presence of five water molecules in excess of those found in the crystal structure (see below). $C_{54}H_{54}N_6NiO_{25}U_2$ (1721.80): calcd. C 37.67, H 3.16, N 4.88; found C 37.76, H 2.87, N 4.73.

$[Ni(bipy)_3][(UO_2)_2(ndc)_3]\cdot DMF\cdot 5H_2O$ (2): 2,6-naphthalenedicarboxylic acid (11 mg, 0.05 mmol), $UO_2(NO_3)_2\cdot 6H_2O$ (25 mg, 0.05 mmol), $Ni(NO_3)_2\cdot 6H_2O$ (15 mg, 0.05 mmol), 2,2′-bipyridine (24 mg, 0.15 mmol), *N*,*N*-dimethylformamide (0.3 mL) and demineralized water (0.8 mL) were placed in a 15 mL tightly closed glass vessel and heated at 140 °C under autogenous pressure, giving light pink crystals of complex **2** in low yield within two weeks.

$[UO_2(ntcma)(H_2O)_2]\cdot 2H_2O$ (3): 1,4,5,8-naphthalenetetracarboxylic acid (16 mg, 0.05 mmol), $UO_2(NO_3)_2\cdot 6H_2O$ (25 mg, 0.05 mmol), $Ni(NO_3)_2\cdot 6H_2O$ (15 mg, 0.05 mmol), 2,2′-bipyridine (24 mg, 0.15 mmol), acetonitrile (0.2 mL) and demineralized water (0.8 mL) were placed in a 15 mL tightly closed glass vessel and heated at 140 °C under autogenous pressure, giving light yellow crystals of complex **3** in low yield, mixed with an amorphous powder, within one week. After separation by hand, a very small quantity of crystals (~2 mg) was subjected to analysis, the results being roughly consistent with retention of half an acetonitrile molecule. $C_{15}H_{13.5}N_{0.5}O_{13}U$ (646.80): calcd. C 27.85, H 2.10, N 1.08; found C 27.85, H 2.02, N 0.36.

$[UO_2Ni(hfdp)(bipy)_2(H_2O)]\cdot H_2O$ (4): 4,4'-(1,1,1,3,3,3-hexafluoroisopropylidene)diphthalic acid (24 mg, 0.05 mmol), $UO_2(NO_3)_2\cdot 6H_2O$ (25 mg, 0.05 mmol), $Ni(NO_3)_2\cdot 6H_2O$ (15 mg, 0.05 mmol), 2,2'-bipyridine (24 mg, 0.15 mmol), *N*-methyl-2-pyrrolidone (0.3 mL), and demineralized water (0.8 mL) were placed in a 15 mL tightly closed glass vessel and heated at 140 °C under autogenous pressure, giving light pink crystals of complex **4** within three days (33 mg, 57% yield). $C_{39}H_{26}F_6N_4NiO_{12}U$ (1153.38): calcd. C 40.61, H 2.27, N 4.86; found C 40.32, H 2.45, N 4.88.

Crystallography: The data were collected at 150(2) K on a Nonius Kappa-CCD area detector diffractometer[67] using graphite-monochromated Mo Kα radiation (λ = 0.71073 Å). The crystals were introduced into glass capillaries with a protective coating of Paratone-N oil (Hampton Research). The unit cell parameters were determined from ten frames, then refined on all data. The data (combinations of φ- and ω-scans with a minimum redundancy of 4 for 90% of the reflections) were processed with HKL2000.[68] Absorption effects were corrected empirically with the program SCALEPACK.[68] The structures were solved by intrinsic phasing with SHELXT,[69] expanded by subsequent difference Fourier synthesis and refined by full-matrix least-squares on F^2 with SHELXL-2014.[70] All non-hydrogen atoms were refined with anisotropic displacement parameters. In complex **1**, the water solvent molecules were given partial occupancies so as to retain acceptable displacement parameters and to account for too close contacts between some of them. The hydrogen atoms of water molecules were found on difference Fourier maps, except for those in **1** and in three water molecules in **2**, and the carbon-bound hydrogen atoms were introduced at calculated positions; all hydrogen atoms were treated as riding atoms with an isotropic displacement parameter equal to 1.2 times that of the parent atom (1.5 for CH_3, with

optimized geometry). Some voids in the lattice of **1** indicate the presence of other, unresolved water solvent molecules, in agreement with elemental analysis results (see above). The highest residual electron density peaks in **4** are located at about 2 Å from the uranium atoms, probably indicating either imperfect absorption corrections or unresolved disorder in the metal coordination sphere. Crystal data and structure refinement parameters are given in Table 1. The molecular plots were drawn with ORTEP-3[71] and the polyhedral representations with VESTA.[72] The topological analyses were made with TOPOS.[73]

CCDC-1573130–1573133 contain the supplementary crystallographic data for this paper. These data can be obtained free of charge from The Cambridge Crystallographic Data Centre via www.ccdc.cam.ac.uk/data_request/cif.

Table 1 Crystal data and structure refinement details

	1	**2**	**3**	**4**
Empirical formula	$C_{54}H_{44}N_6NiO_{20}U_2$	$C_{69}H_{59}N_7NiO_{22}U_2$	$C_{14}H_{12}O_{13}U$	$C_{39}H_{26}F_6N_4NiO_{12}U$
M (g mol^{-1})	1631.72	1873.00	626.27	1153.38
Crystal system	orthorhombic	monoclinic	monoclinic	triclinic
Space group	*Pnna*	$P2_1/n$	$P2_1/c$	$P\bar{1}$
a (Å)	17.2556(3)	16.2231(5)	5.7020(2)	10.9429(5)
b (Å)	13.6441(4)	22.3002(4)	10.1628(3)	16.5626(12)
c (Å)	28.5214(9)	18.4139(5)	29.0906(11)	23.8063(17)
α (°)	90	90	90	81.005(3)
β (°)	90	99.8152(16)	91.577(2)	78.747(4)
γ (°)	90	90	90	74.767(4)
V (Å^3)	6715.0(3)	6564.2(3)	1685.11(10)	4057.8(5)
Z	4	4	4	4
ρ_{calcd} (g cm^{-3})	1.614	1.895	2.469	1.888
μ(Mo-K$_\alpha$) (mm^{-1})	5.158	5.292	9.706	4.545
F(000)	3128	3640	1168	2232
Reflections collected	141520	197488	52449	171770
Independent reflections	6369	12456	4355	15377
Observed reflections [$I > 2\sigma(I)$]	5168	10170	3943	10810
R_{int}	0.024	0.035	0.028	0.073
Parameters refined	409	912	253	1135
R_1	0.033	0.033	0.026	0.048
wR_2	0.099	0.078	0.063	0.132
S	1.068	1.026	1.122	1.005
$\Delta\rho_{min}$ (e Å^{-3})	–1.22	–1.32	–1.33	–1.50
$\Delta\rho_{max}$ (e Å^{-3})	0.89	1.93	1.56	4.20

Luminescence measurements: Emission spectra for compounds **1** and **4** were recorded on solid samples using a Horiba-Jobin-Yvon Fluorolog spectrofluorometer. The powdered complex was pressed between two silica plates which were mounted such that the faces were oriented vertically and at 45° to the incident excitation radiation. An excitation wavelength of 420 nm was used in all cases and the emissions monitored between 450 and 650 nm. The very low yield of the synthesis of **2** and the presence of amorphous material accompanying complex **3** prevented luminescence measurements on these compounds.

Acknowledgment

We thank Pr. B. Masci for the provision of the unique tetracarboxylate ligand used in this work.

References

[1] M. B. Andrews, C. L. Cahill, *Chem. Rev*. **2013**, *113*, 1121–1136.

[2] T. Loiseau, I. Mihalcea, N. Henry, C. Volkringer, *Coord. Chem. Rev.* **2014**, *266–267*, 69–109.

[3] J. Su, J. S. Chen, *Struct. Bond*. **2015**, *163*, 265–296.

[4] C. R. Groom, I. J. Bruno, M. P. Lightfoot, S. C. Ward, *Acta Crystallogr., Sect. B* **2016**, *72*, 171–179.

[5] P. Thuéry, J. Harrowfield, *Cryst. Growth Des.* **2014**, *14*, 4214–4225.

[6] P. Thuéry, E. Rivière, J. Harrowfield, *Inorg. Chem.* **2015**, *54*, 2838–2850.

[7] P. Thuéry, J. Harrowfield, *Inorg. Chem.* **2015**, *54*, 10539–10541.

[8] P. Thuéry, *Cryst. Growth Des.* **2016**, *16*, 546–549.

[9] P. Thuéry, J. Harrowfield, *Inorg. Chem.* **2016**, *55*, 2133–2145.

[10] P. Thuéry, E. Rivière, J. Harrowfield, *Cryst. Growth Des.* **2016**, *16*, 2826–2835.

[11] P. Thuéry, J. Harrowfield, *Cryst. Growth Des.* **2017**, *17*, 2116–2130.

[12] Z. T. Yu, G. H. Li, Y. S. Jiang, J. J. Xu, J. S. Chen, *Dalton Trans.* **2003**, 4219–4220.

[13] Z. L. Liao, G. D. Li, M. H. Bi, J. S. Chen, *Inorg. Chem.* **2008**, *47*, 4844–4853.

[14] W. Yang, T. Tian, H. Y. Wu, Q. J. Pan, S. Dang, Z. M. Sun, *Inorg. Chem.* **2013**, *52*, 2736–2743.

[15] W. Yang, S. Dang, H. Wang, T. Tian, Q. J. Pan, Z. M. Sun, *Inorg. Chem.* **2013**, *52*, 12934–12402.

[16] H. H. Li, X. H. Zeng, H. Y. Wu, X. Jie, S. T. Zheng, Z. R. Chen, *Cryst. Growth Des.* **2015**, *15*, 10–13.

[17] P. Thuéry, *Inorg. Chem.* **2013**, *52*, 435–447.

[18] P. Thuéry, *Eur. J. Inorg. Chem.* **2014**, 58–68.

[19] P. Thuéry, *Inorg. Chem. Commun.* **2015**, *59*, 25–27.

[20] P. Thuéry, J. Harrowfield, *Inorg. Chem.* **2015**, *54*, 6296–6305.

[21] P. Thuéry, J. Harrowfield, *Inorg. Chem.* **2015**, *54*, 8093–8102.

[22] P. Thuéry, J. Harrowfield, *CrystEngComm* **2016**, *18*, 1550–1562.

[23] J. Y. Kim, A. J. Norquist, D. O'Hare, *Dalton Trans.* **2003**, 2813–2814.

[24] I. Mihalcea, N. Henry, N. Clavier, N. Dacheux, T. Loiseau, *Inorg. Chem.* **2011**, *50*, 6243–6249.

[25] I. Mihalcea, N. Henry, T. Bousquet, C. Volkringer, T. Loiseau, *Cryst. Growth Des.* **2012**, *12*, 4641–4648.

[26] J. Olchowka, C. Falaise, C. Volkringer, N. Henry, T. Loiseau, *Chem. – Eur. J.* **2013**, *19*, 2012–2022.

[27] I. Mihalcea, N. Henry, T. Loiseau, *Eur. J. Inorg. Chem.* **2014**, 1322–1332.

[28] M. S. Grigor'ev, I. A. Charushnikova, A. M. Fedoseev, *Radiochem*. **2015**, *57*, 483–487.

[29] X. S. Zhai, W. G. Zhu, W. Xu, Y. J. Huang, Y. Q. Zheng, *CrystEngComm* **2015**, *17*, 2376–2388.

[30] X. Gao, C. Wang, Z. F. Shi, J. Song, F. Y. Bai, J. X. Wang, Y. H. Xing, *Dalton Trans.* **2015**, *44*, 11562–11571.

[31] C. Falaise, J. Delille, C. Volkringer, H. Vezin, P. Rabu, T. Loiseau, *Inorg. Chem.* **2016**, *55*, 10453–10466.

[32] Y. B. Go, X. Wang, A. J. Jacobson, *Inorg. Chem.* **2007**, *46*, 6594–6600.

[33] Y. Xia, K. X. Wang, J. S. Chen, *Inorg. Chem. Commun.* **2010**, *13*, 1542–1547.

[34] S. G. Thangavelu, M. B. Andrews, S. J. A. Pope, C. L. Cahill, *Inorg. Chem.* **2013**, *52*, 2060–2069.

[35] S. G. Thangavelu, C. L. Cahill, *Cryst. Growth Des.* **2016**, *16*, 42–50.

[36] P. Thuéry, B. Masci, J. Harrowfield, *Cryst. Growth Des.* **2013**, *13*, 3216–3224.

[37] P. Thuéry, *CrystEngComm* **2009**, *11*, 1081–1088.

[38] L. Z. Zhu, C. Z. Wang, L. Mei, L. Wang, Y. H. Liu, Z. T. Zhu, Y. L. Zhao, Z. F. Chai, W. Q. Shi, *CrystEngComm* **2015**, *17*, 3031–3040.

[39] A. C. Blackburn, L. J. Fitzgerald, R. E. Gerkin, *Acta Crystallogr., Sect. C* **1997**, *53*, 1991–1995 and references therein.

[40] A. L. Spek, *Acta Crystallogr., Sect. D* **2009**, *65*, 148–155.

[41] M. A. Spackman, D. Jayatilaka, *CrystEngComm* **2009**, *11*, 19–32, and references therein.

[42] S. K. Wolff, D. J. Grimwood, J. J. McKinnon, M. J. Turner, D. Jayatilaka, M. A. Spackman, *CrystalExplorer*, University of Western Australia, 2012.

[43] R. Taylor, O. Kennard, *J. Am. Chem. Soc.* **1982**, *104*, 5063–5070.

[44] G. R. Desiraju, *Acc. Chem. Res.* **1996**, *29*, 441–449.

[45] A. Gavezzotti, *CrystEngComm* **2013**, *15*, 4027–4035.

[46] L. Mei, C. Z. Wang, L. Z. Zhu, Z. Q. Gao, Z. F. Chai, J. K. Gibson, W. Q. Shi, *Inorg. Chem.* **2017**, *56*, 7694–7706.

[47] Z. T. Yu, Z. L. Liao, Y. S. Jiang, G. H. Li, J. S. Chen, *Chem. – Eur. J.* **2005**, *11*, 2642–2650.

[48] P. Thuéry, E. Rivière, *Dalton Trans.* **2013**, *42*, 10551–10558.

[49] L. Liang, Y. Cai, X. Li, R. Zhang, J. Zhao, C. Liu, N. S. Weng, *Z. Anorg. Allg. Chem.* **2015**, *641*, 1744–1748.

[50] E. Cole, E. Flores, M. Basile, A. Jayasinghe, J. de Groot, D. K. Unruh, T. Z. Forbes, *Polyhedron*, **2016**, *114*, 378–384.

[51] P. Thuéry, J. Harrowfield, *Inorg. Chem.* **2016**, *55*, 6799–6816.

[52] P. Thuéry, J. Harrowfield, *Cryst. Growth Des.* **2017**, *17*, 963–966.

[53] P. Thuéry, J. Harrowfield, *Inorg. Chem.* **2017**, *56*, 1455–1469.

[54] G. R. Desiraju, R. Parthasarathy, *J. Am. Chem. Soc.* **1989**, *111*, 8725–8726.

[55] K. P. Carter, C. L. Cahill, *Inorg. Chem. Front.* **2015**, *2*, 141–156.

[56] K. P. Carter, M. Kalaj, C. L. Cahill, *Inorg. Chem. Front.* **2017**, *4*, 65–78.

[57] M. Kalaj, K. P. Carter, A. V. Savchenkov, M. M. Pyrch, C. L. Cahill, *Inorg. Chem.* **2017**, *56*, 9156–9168.

[58] K. E. Knope, D. T. de Lill, C. E. Rowland, P. M. Cantos, A. de Bettencourt-Dias, C. L. Cahill, *Inorg. Chem.* **2012**, *51*, 201–206.

[59] A. Brachmann, G. Geipel, G. Bernhard, H. Nitsche, *Radiochim. Acta* **2002**, *90*, 147–153.

[60] A. T. Kerr, C. L. Cahill, *Cryst. Growth Des*. **2014**, *14*, 1914–1921.

[61] P. Thuéry, J. Harrowfield, *Inorg. Chem*., DOI: 10.1021/acs.inorgchem.7b02176.

[62] M. P. Redmond, S. M. Cornet, S. D. Woodall, D. Whittaker, D. Collison, M. Helliwell, L. S. Natrajan, *Dalton Trans.* **2011**, *40*, 3914–3926.

[63] L. S. Natrajan, *Coord. Chem. Rev.* **2012**, *256*, 1583–1603.

[64] P. Thuéry, J. Harrowfield, *Cryst. Growth Des*. **2014**, *14*, 1314–1323.

[65] R. G. Surbella, III, M. B. Andrews, C. L. Cahill, *J. Solid State Chem.* **2016**, *236*, 257–271.

[66] N. P. Martin, C. Falaise, C. Volkringer, N. Henry, P. Farger, C. Falk, E. Delahaye, P. Rabu, T. Loiseau, *Inorg. Chem.* **2016**, *55*, 8697−8705.

[67] R. W. W. Hooft, *COLLECT*, Nonius BV: Delft, The Netherlands, 1998.

[68] Z. Otwinowski, W. Minor, *Methods Enzymol.* **1997**, *276*, 307–326.

[69] G. M. Sheldrick, *Acta Crystallogr., Sect. A* **2015**, *71*, 3–8.

[70] G. M. Sheldrick, *Acta Crystallogr., Sect. C* **2015**, *71*, 3–8.

[71] L. J. Farrugia, *J. Appl. Crystallogr.* **1997**, *30,* p. 565.

[72] K. Momma, F. Izumi, *J. Appl. Crystallogr.* **2008**, *41*, 653–658.

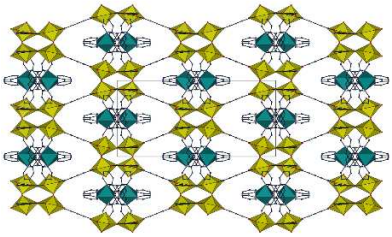
[73] V. A. Blatov, *TOPOS*, Samara State University, Russia, 2004.

Table of Contents Entry

Complexes of Uranyl Ions with Aromatic di- and tetra-Carboxylates Involving $[Ni(bipy)_n]^{2+}$ (n = 2, 3) Counter-Ions

Pierre Thuéry and Jack Harrowfield

Key Topic: Uranyl-Based Network Solids



Four di- and tetracarboxylate ligands based on aromatic platforms have been used to synthesize four uranyl ion complexes under solvo-hydrothermal conditions and in the presence of nickel(II) cations and 2,2′-bipyridine. All four complexes crystallize as two-dimensional networks with the hcb or fes topologies. Interactions in the lattices have been analyzed through examination of Hirshfeld surfaces, and uranyl emission spectra are given in two cases.